Carbohydrate Polymers 84 (2011) 1133–1140

Contents lists available at ScienceDirect

Carbohydrate Polymers

journal homepage: www.elsevier.com/locate/carbpol

Cryo-milling of starch granules leads to differential effects on molecular size and conformation

Sushil Dhital, Ashok K. Shrestha, Bernadine M. Flanagan, Jovin Hasjim, Michael J. Gidley*

Centre for Nutrition and Food Sciences, The University of Queensland, Brisbane, Qld 4072, Australia

ARTICLE INFO

Article history:
Received 9 December 2010
Accepted 4 January 2011
Available online 8 January 2011

Keywords:
Starch granules
Cryo-milling
Granule
Amylose
Amylopectin
Crystallinity
Molecular size

ABSTRACT

Milling of starch granules is important for many food applications and involves a combination of mechanical and thermal energy. In order to understand the effects of mechanical force alone, four commercial starches including maize starch (MS), potato starch (PS), and two high amylose maize starches (HAMS) (Gelose 50 and Gelose 80) were cryo-milled for 20 min under the same conditions. The structural and conformational changes of the starches after cryo-milling were evaluated using X-ray diffraction, NMR spectroscopy, IR and Raman spectroscopy, and size exclusion chromatography (SEC). The cryo-milled starches had less crystallinity (15–35%) and 35–50% less ordered structure (double and single helices) than the native starch counterparts. The gelatinisation temperatures of the starches were not significantly altered by cryo-milling, but the gelatinisation enthalpies were significantly reduced in line with the reductions in the amount of double helices. Although, all four starches showed similar extent of degradation of crystalline/ordered structure, SEC results showed a greater degradation of amylopectin molecule in MS and PS than in HAMS. Increased amylose content in starch seemed to reduce the molecular degradation during milling, which is consistent with a role for amylose as a mechanical plasticiser in starch granules. It is concluded that (i) cryo-milling has differential effects on molecular size and conformation depending on starch granule type, and (ii) deterioration of starch crystalline and molecular order by mechanical treatment is not necessarily linked with the reduction in molecular size. The implication from the results is that the mechanical forces acting during cryo-milling are capable of disrupting helical and crystalline structures without breaking covalent bonds of starch molecules.

1. Introduction

Application of physical force damages starch granules, both by breaking them into smaller particles and by disrupting internal granule architecture. This is a common phenomenon during milling or extraction of flour from starchy grains or tubers. Ball milling has been extensively used to study the properties of damaged starch at the laboratory scale. Starch damaged by ball milling is known to possess altered granule structure, physicochemical properties, and enzyme digestibility, depending on the types and the severity of the treatments, as well as the sources of starch. These changes are thought to be due to progressive breakage of both covalent and hydrogen bonds between AP clusters in crystalline regions resulting in gelatinisation of starch granules on subsequent hydration (Morrison, Tester, & Gidley, 1994; Yamada, Tamaki, & Hisamatsu, 1997). Ball-milled starch granules are less birefringent than native starch granules with reduction in crystallinity, number of double helices, and gelatinisation enthalpy, suggesting that semi-crystalline granules are progressively converted into an amorphous state (Chen, Lii, & Lu, 2003; Huang, Lu, Li, & Tong, 2007; Morrison & Tester, 1994; Morrison et al., 1994; Tamaki, Hisamatsu, Teranishi, & Yamada, 1997; Tamaki, Hisamatsu, Teranishi, Adachi, & Yamada, 1998; Tester, 1997). Waxy starch granules are damaged more easily than normal starch granules (Tester, 1997), probably because amylose in the amorphous regions of non-waxy starches acts as a shock absorber and provides a cushioning effect limiting amylopectin breakdown during milling (Han, Campanella, Mix, & Hamaker, 2002). At low temperature (<60 °C) damaged starch granules swell more upon hydration than intact starch granules. At higher temperatures, damaged starch granules, however, have a lower swelling factor resulting in differences in the pasting properties of milled starch (Becker, Hill, & Mitchell, 2001; Han et al., 2002; Tester & Morrison, 1994; Tester, 1997). During ball milling, starch granules are subjected to physical force as well as thermal

Abbreviations: MS, maize starch; PS, potato starch; HAMS, high amylose maize starch; G50, Gelose 50; G80, Gelose 80; AM, amylose; AP, amylopectin; NMR, nuclear magnetic resonance; FTIR, Fourier transformed infrared; SEC, size exclusion chromatography; DMSO, dimethyl sulphoxide; R_h, hydrodynamic radius (nm); V_h, hydrodynamic volume (nm^3); DSC, differential scanning calorimeter; ΔH, change in enthalpy of gelatinisation (J/g); T_o, gelatinisation onset temperature (°C); T_p, gelatinisation peak temperature (°C); T_c, gelatinisation conclusion temperature (°C).

* Corresponding author. Tel.: +61 7 33652145; fax: +61 7 33651177.
E-mail addresses: m.gidley@uq.edu.au, mike.gidley@uq.edu.au (M.J. Gidley).

0144-8617/$ – see front matter © 2011 Elsevier Ltd. All rights reserved.
doi:10.1016/j.carbpol.2011.01.002

energy (heat) that is generated by the impact of grinding balls. Thus, the changes in physicochemical properties of ball-milled starches are due to the combined effects of the thermal and mechanical treatments.

Cryo-milling, a dry milling process under liquid nitrogen bath, was used in this study to mill starch granules. Milling at the cryogenic temperature prevents the starch granules from heat damage. Few studies have reported the properties of cryo-milled starches. The cryo-milled rice starch had less crystallinity, higher water absorption, and higher water solubility compared to native rice starches (Devi, Fibrianto, Torley, & Bhandari, 2009). In the preceding paper (Dhital, Shrestha, & Gidley, 2010), we evaluated the effects of cryo-milling on the susceptibility to *in vitro* amylase digestion and the functional properties of maize starch, potato starch, and high amylose maize starches (HAMS). The results showed that, although cryo-milling had a major effect on starch digestibility, it did not convert slowly digestible PS and HAMS into a rapidly digestible type similar to normal maize starch, emphasizing the role of granule-level structure in controlling enzyme hydrolysis rates. We now describe the changes in molecular and supra-molecular structure of cryo-milled starches varying in plant origins, to further elucidate the effects of physical forces on the starch granules with varying amylose contents and crystalline structures.

By comparing the relative responses from diverse types of starch granules to the same cryo-milling procedure, we aim to define which levels of structural organisation respond similarly for all starch types, and which show origin-specific effects. In particular, the relative effects of cryo-milling on starches in terms of molecular structure (as monitored by size exclusion chromatography before and after debranching) and conformation or supra-molecular structure (as monitored by X-ray diffraction, NMR, IR and Raman spectroscopies) will be discussed.

2. Materials and methods

2.1. Materials

Potato starch (PS, S4251) was purchased from Sigma–Aldrich, Castle Hill, NSW, Australia. Normal maize starch (MS), Gelose 50 (G50) and Gelose 80 (G 80) were purchased from Penford Australia Ltd., Lane Cove, NSW, Australia. MS, PS, G50, and G80 have 27.1, 22.2, 57.5, and 83.6% amylose, respectively (Dhital et al., 2010). All starches were cryo-milled in a liquid nitrogen bath (Freezer/Mill 6850 SPEX, Metuchen, NJ, USA) for 20 min at a milling speed of 10 s^{-1}. Damaged starch contents of the cryo-milled MS, PS, G50 and G80 (abbreviated as MSCM, PSCM, G50CM and G80CM) were 24.7, 22.9, 13.4 and 10.2%, respectively (Dhital et al., 2010). The water contents of all starch samples, both native (unmilled) and cryo-milled were adjusted via vapour phase isopiestic equilibration over saturated K_2CO_3 salt solution at 20 °C for one week, providing an environment with a relative humidity of 44%. The resulting moisture contents of all conditioned starch samples were within the range 9–12% (w/w).

2.2. X-ray diffractometry

X-ray diffraction (XRD) analysis was performed using a X-ray diffractometer (D8 Advance, Bruker AXS GmbH, Karlsruhe, Germany) operating at 40 kV and 30 mA with Cu Kα1 radiation (λ) as 0.15405 nm. The scanning region was set from 3° to 40° of the diffraction angle 2θ, which covers all the significant diffraction peaks of starch crystallites. A step interval of 0.02° and a scan rate of 0.5°/min were employed for all samples. The percentage of crystallinity was calculated as the ratio of the total peak area to the total diffraction area (two-phase model) (Htoon et al., 2009; Lopez-Rubio, Flanagan, Gilbert, & Gidley, 2008). The diffractograms were smoothed by 13 points using Traces version 3.01 software (Diffraction Technology Pty LTD, Mitchell, ACT, Australia) before calculating the percentage of crystallinity.

2.3. ^{13}C solid state nuclear magnetic resonance spectroscopy

Starch samples were analyzed by solid-state ^{13}C CP/MAS nuclear magnetic resonance (NMR) spectroscopy (Bruker MSL-300 spectrometer, Bruker, Karlsruhe, Germany) using the spectral acquisition and interpretation methodology described elsewhere (Tan, Flanagan, Halley, Whittaker, & Gidley, 2007). This method provides quantitative analyses of double helices, single helices, and amorphous conformational features within solid starch samples.

2.4. Fourier transform infrared spectroscopy

Fourier transformed infrared (FTIR) spectra of starch samples were recorded on a FTIR spectrometer (Nicolet 5700, Thermo Electron Corporation, Madison, WI, USA) using an attenuated total reflectance (ATR) single reflectance cell with a diamond crystal. For each spectrum, 32 scans were recorded over the range of 1200–800 cm^{-1} at room temperature (about 22 °C) at a resolution of 4 cm^{-1}, co-added and Fourier transformed. The background spectrum was recorded on air and subtracted from the sample spectrum. The ratio of absorbance at wave numbers 1045/1022 was calculated to represent ordered short range starch structures (vanSoest, Tournois, deWit, & Vliegenthart, 1995).

2.5. Fourier transform-Raman spectroscopy

Fourier transform-Raman (FT-Raman) spectra were performed on an FT-Raman Module (NXR, Thermo Fisher Scientific, Madison, WI, USA). The Raman optics system comprised a Nd:YVO_4 laser operating at 1064 nm, sample holders, an InGaAs (Indium-Gallium Arsenide) detector, and a CaF_2 beam splitter. Spectra of starches placed in the sample holder were collected with a laser power of 0.77–0.82 W, a mirror velocity of 0.3165 cm s^{-1}, and 256 scans at a resolution of 16 cm^{-1}. Spectra were obtained in the Raman shift range between 400 and 4000 cm^{-1} using OMNIC software (version 5.1, Thermo Electron Corporation, Madison, WI, USA).

2.6. Size exclusion chromatography

The molecular size distributions of native and cryo-milled starches were analyzed using a size exclusion chromatography (SEC) system (Agilent 1100 Series, Agilent Technologies, Waldbronn, Germany) equipped with a refractive index detector (RID-10A, Shimadzu, Kyoto, Japan) following the method of Cave, Seabrook, Gidley, & Gilbert (2009). For whole (fully branched) size distribution, starch (2 mg) was dissolved in DMSO solution (1 mL) containing 0.5% (w/w) LiBr (DMSO/LiBr) at 80 °C in a thermomixer (Thermomixer Comfort, Eppendorf, Hamburg, Germany) for 24 h. For debranched size distribution, starch (4 mg) was dissolved in DMSO/LiBr (1 mL) in the same way as the fully branched sample. The dissolved starch in DMSO/LiBr was then precipitated using 3 mL absolute ethanol. The recovered starch pellet was dissolved in 0.9 mL deionised water in a boiling water bath for 15 min. After being cooled to room temperature, the starch dispersion was mixed with 20 μL sodium azide solution (100 mg/mL), 1 mL acetate buffer (0.1 M, pH 3.5), and 2 μL isoamylase, in sequence, and the debranching reaction was carried out at 37 °C for 3 h. The debranched starch was precipitated with 5 mL absolute ethanol, centrifuged (4000 × *g*, 10 min), and dissolved in 1 mL DMSO/LiBr at 80 °C in the thermomixer for 3 h. DMSO/LiBr was used as eluent and the flow rate was set at 0.3 and 0.6 mL/min for fully branched and debranched

starch size distribution analyses, respectively. The detector was set at 45 °C. A series of pullulan standards (Polymer Standard Services, Mainz, Germany) with varying molecular weights ranging from 342 to 2,350,000 Da were used for calibration. The resulting SEC chromatograms were analyzed using PSS WinGPC Unity software (Polymer Standard Services, Mainz, Germany) and normalised to yield the same peak height of amylose. The size distribution [$w \log(V_h)$] was calculated from the detector signal and plotted against log (R_h/nm) following the method of Cave et al. (2009) where R_h is the hydrodynamic radius (nm) calculated from hydrodynamic volume V_h with $V_h = 4/3\pi R_h^3$.

As discussed by Cave et al. (2009), presenting the SEC distribution as a function of R_h (or V_h), which is a molecular quantity independent of machine set-up, enables these data to be reproduced, whereas presenting such data as elugrams in terms of elution time or volume cannot, because the elution varies with the particular machine set-up and even from day-to-day with a given set-up. The SEC distributions used for comparison here were run on the same day to avoid day-to-day variations of the SEC instrument. Although it is unavoidable that the amylopectin component suffers some shear damage in SEC (Cave et al., 2009), as long as the comparison is made with samples run on the same day, this shear will be the same for every sample, and so the resulting distributions can be meaningfully compared (Syahariza, Li, & Hasjim, 2010).

2.7. Differential scanning calorimetry

The gelatinisation properties of starch samples were analyzed using a differential scanning calorimeter (DSC 1, Mettler Toledo, Schwerzenbach, Switzerland). Each sample (4 ± 0.1 mg) was mixed with (12 ± 0.3 mg) deionised water in a DSC pan (aluminium-low pressure, 40 μL), which was then hermetically sealed. The pans were held at 10 °C for 5 min and then heated to 120 °C at 5 °C/min. The onset (T_o), peak (T_p), and conclusion temperatures (T_c), and the enthalpy of gelatinisation (ΔH) were determined using the built-in software (STARe System, Mettler Toledo, Schwerzenbach, Switzerland).

2.8. Statistical analysis

Results were expressed as means with standard deviation in parentheses from at least duplicate measurements, except for XRD and NMR, where only single experiments were performed. Analysis of variance (ANOVA) was used to determine the least significance at $p \leq 0.05$ using Genstat 5 (Release 3.2, Lawes Agricultural Trust, Harpenden, Hertfordshire, UK).

3. Results and discussion

3.1. Starch crystallinity and molecular order

X-ray diffraction is used to study the change in starch crystallinity brought about by physical treatment of granular starch. As expected, native MS exhibited the A-type diffraction pattern with major peaks at ~15, 17, 18 and 23° 2θ, whereas native PS and HAMS had the B-type patterns with distinct peaks at ~5, 17, 22 and 24° 2θ (Fig. 1). A small V-type diffraction peak was also observed at 20° 2θ for MS and HAMS which was associated with orderly packed amylose single helical complexes with lipid (Zobel, 1964). The cryo-milled starches had decreased intensities of diffraction peaks thus the decrease in calculated percentage of crystallinity (Table 1) suggesting that physical force in the absence of thermal energy is sufficient to disrupt the crystalline structure of clustered amylopectin. The crystallinity values of high-amylose starches are less affected by milling (15–20% reduced cf 30–35% reduced for PS and MS – Table 1). This might be due to the lower crystallinity in native HAMS starch granules and/or the abundant amylose providing a cushioning effect towards physical force (Han et al., 2002). The decrease in crystallinity was in the order of PS > MS > HAMS, which was positively correlated ($r = 0.99$, $p < 0.01$) with the damaged starch contents.

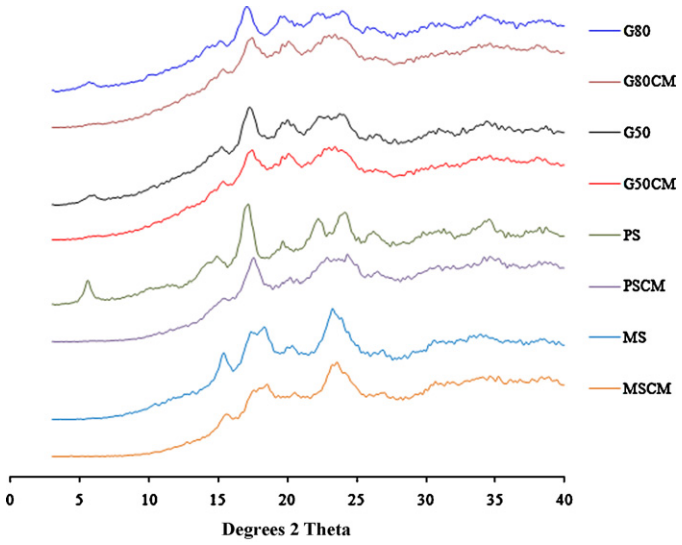

Fig. 1. X-ray diffractograms of native and cryo-milled starches.

Close observation of the diffraction peaks (Fig. 1) revealed that the peaks corresponding to smaller angles and, hence, larger interplanar spacing (d-spacing) were more affected by milling than the peaks corresponding to smaller d-spacing values. For example, the non-overlapping prominent peak at ~5° 2θ (d-spacing ~17 Å) for PS and HAMS completely disappeared after milling, but there was only a slight reduction in the intensities of peaks at 22° and 24° 2θ (d-spacings ~4 and 3.7 Å). Similarly, the intensity of peak at 15° 2θ for MS was reduced to a greater extent than the other peaks, suggesting that the disappearance of the 5° 2θ peak for the B-type starches was not an exfoliation effect. We propose that the selective loss or broadening of peaks reflects a marked disruption of crystallites upon cryo-milling, with greater effects for the diffraction peaks of longer d-spacings. In addition, the C-type pattern was observed in the cryo-milled PS and HAMS, specifically the peaks at 22–24° 2θ overlapped with each other forming a single peak. Thus, prolonged cryo-milling of the B-type starches will lead to the formation of C-type conformation, and, finally, to an amorphous form without distinct diffraction peaks. All crystallinity was lost when rice starch was cryo-milled continuously for 60 min (Devi et al., 2009), a more extensive treatment than used in the present study.

In accordance with the XRD findings, there was a considerable change in the double helix and single helix contents in the cryo-milled starches (Table 1), obtained from comparing the area of C1 (90–110 ppm) signals in the ordered NMR sub-spectrum relative to the area of C1 signals in the starch NMR total spectrum. Fig. 2A shows, as an example, the amorphous and ordered sub-spectra, together with the original spectrum of G50 HAMS, and Fig. 2B compares the spectra of starches before and after cryo-milling. In all cases, the shape of the C1 signal changed towards that of amorphous starch after cryo-milling. Quantifications of these changes in all starches (Tan et al., 2007) are summarized in Table 1. The decrease in the double helices after milling was greater (35–50%) than the decrease in the crystallinity (15–35%) for all starches. Fundamentally, starch double helices are stable as the two chains fit together compactly with the hydrophobic zones of monomer units from the two chains in close contact, and the hydroxyl groups located for strong inter-chain hydrogen bonding. Although the

Table 1
Crystallinity and molecular order of native and cryo-milled starches.

Starch	XRD[a] (%)	NMR[a]			FTIR[a,b] (1045/1022 ratio)
		Single helices (%)	Double helices (%)	Amorphous (%)	
MS	25.5	2.7	28.6	68.4	0.70
MSCM	17.2	2.1	13.7	84.1	0.68
PS	26.4	1.9	30.1	67.9	0.72
PSCM	17.8	1.3	19.6	79.0	0.69
G50	19.3	3.9	21.8	74.2	0.68
G50CM	15.8	2.3	13.1	84.5	0.66
G80	18.3	7.8	19.8	72.3	0.67
G80CM	15.2	3.1	11.1	85.6	0.66

[a] XRD, NMR and FTIR values are within CV of 5%.
[b] Ratio of the bands at 1045 cm^{-1} and 1022 cm^{-1}.

disruption of double helical structures within starch granules is normally achieved by thermal gelatinisation (e.g. 60–70 °C in excess water), in this study it was clearly shown that the disruption could be achieved by input of mechanical energy at low temperatures, such as cryo-milling. The greater relative decrease in double helices than crystallinity suggests that the breakage of starch granules during cryo-milling occurs not only in true crystalline regions but also in the less ordered regions as not all double helices in the starch granules are involved in the forming of crystalline structure (Cooke & Gidley, 1992; Lopez-Rubio et al., 2008).

The infrared spectra and the ratios of absorbance at 1045 and 1022 cm^{-1} for the native and cryo-milled starches are displayed in Fig. 3A and Table 1, respectively. The bands at 1047 (1045) and 1022 cm^{-1} have been associated with ordered (organised) and amorphous (less organised) structures in starch and their absorbance ratio can be used as an index to characterize the short-range alignment of helices (vanSoest et al., 1995). The ATR IR technique can give spectral information up to ~2 μm in depth for starch granules representing several growth rings (~0.1 μm) (Sevenou, Hill, Farhat, & Mitchell, 2002). In parallel with the XRD and NMR data, the decrease in the 1045/1022 cm^{-1} ratio (Table 1) of the cryo-milled starches indicates a decrease in the molecular order, which is likely to be associated with the disruption of double helices by milling. However, the decrease in this ratio (~5%) is less pronounced than the decreases in crystallinity (15–35%) and double helices (35–50%). Similar information might be potentially obtained from FT-Raman spectra, but the data interpretation is hampered by limited spectral assignments. The Raman spectra of the cryo-milled samples showed less intensity for bands at 478 cm^{-1} (Fig. 3B, bold arrow), a dominating skeletal vibration mode of the pyranose ring (Bulkin, Kwak, & Dea, 1987). Although this might be due to the breakage of glucan chains during milling, it may also reflect local conformational or dynamic changes. The Raman band at 1260 cm^{-1} (Fig. 3B, dashed arrow) is due to a CH_2OH associated with the deformation assigned to V-form amylose (Cael, Koenig, & Blackwell, 1975; Santha, Sudha, Vijayakumari, Nayar, & Moorthy, 1990). The cryo-milled HAMS showed a less intense band at 1260 cm^{-1}, suggesting a possible disruption of V-amylose, consistent with the NMR spectral analysis (Table 1). Intensity differences in the 2800–3000 cm^{-1} range could be attributed to the variations in the amount of amylose and amylopectin among starches (Kizil, Irudayaraj, & Seetharaman, 2002).

Mechanical forces act simultaneously upon starch granules as a single event or multiple events, e.g. during ball milling (Morrison et al., 1994) or cryo-milling, fracturing the granules into different smaller particles of random sizes (fractions) as observed by electron microscopy (Dhital et al., 2010), and reducing ordered structure within (fractured) granules. The results show that the starch granules with greater crystallinity and/or lower amylose content are more susceptible to damage in their ordered structures (Table 1).

3.2. Molecular size distribution of starch

The size distribution of fully branched native MS, PS and HAMS showed two broad, but well resolved, peaks assigned to amylose (AM) and amylopectin (AP) fractions (Fig. 4). Although this is a simplistic assignment, it is consistent with the amylose contents of the starches as determined by iodine colorimetry. Cryo-milling seemed to cause some breakage of AP to smaller molecules which were co-eluted with the AM resulting in an apparent increase in the ratio of AM to AP peaks of the cryo-milled starch compared with the native (unmilled) starches. The size distributions (Fig. 4) were normalised to the 'amylose' peak so that a decrease in peak area of AP could be easily observed. The relative decrease in the AP peak area was greater for the starches with higher AP content, i.e. MS and PS showing greater decrease compared to HAMS, suggesting the

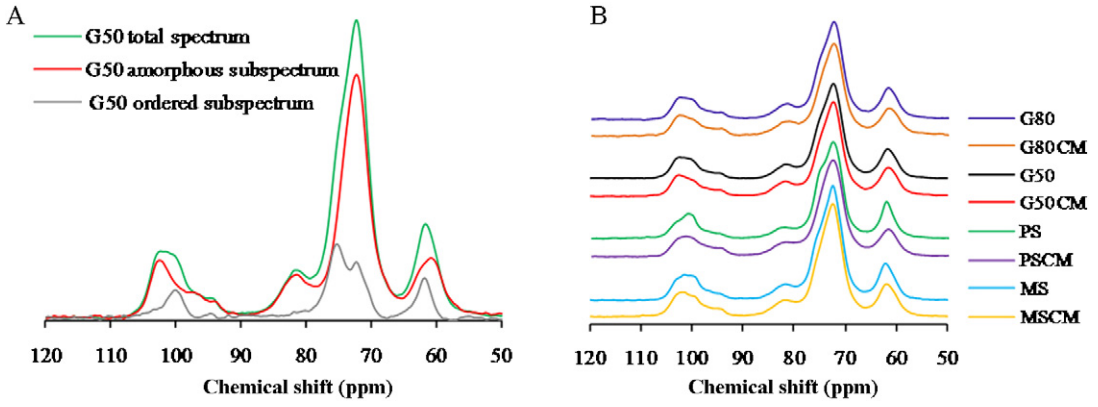

Fig. 2. ^{13}C CP/MAS NMR spectra of G50 showing ordered and amorphous sub-spectra (A) and total spectra of native and cryo-milled starches (B).

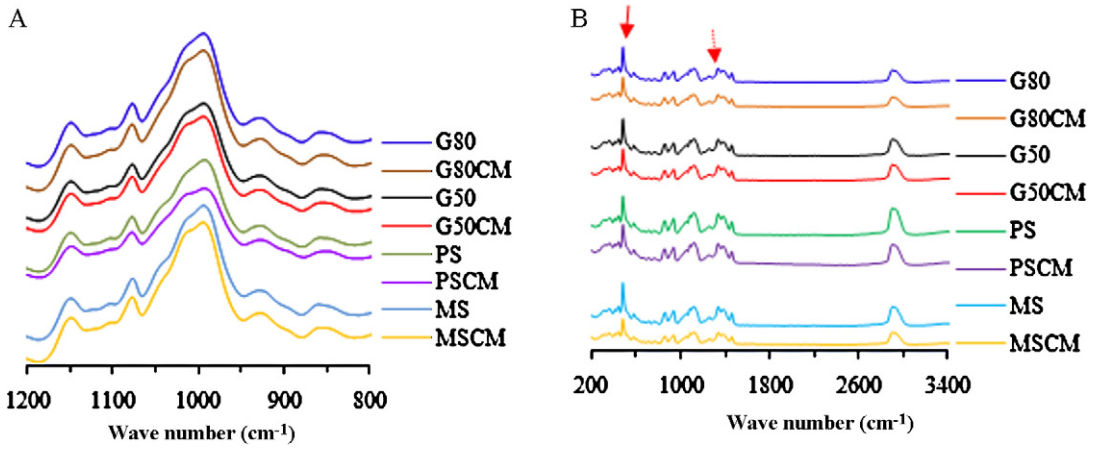

Fig. 3. A. Fourier transform infrared spectra of native and cryo-milled starches; B. Fourier transform Raman spectra of native and cryo-milled starches. Highlighted bands at 478 and 1260 cm^{-1} are discussed in the text.

protective role of amylose against molecular degradation by physical force. Although the trend in the molecular size reduction upon cryo-milling appears to approximately correlate with the relative changes in the crystallinity and double helix contents (Table 1), the extent of the molecular degradation (Fig. 4) was minor compared with the loss of ordered structure after cryo-milling (Table 1). In particular, for Gelose 80, there was no detectable difference in molecular size distributions before and after cryo-milling (Fig. 4D), but marked reduction in the ordered structure levels was observed (Fig. 1 and Table 1). The size distributions of fully branched starch, to a limited extent, also provide information about degradation points within the AP molecules. If the outer chains of AP were cleaved during milling, the resulting SEC profile would have a separate peak at molecular size smaller than AM associated with the short AP branches. However, the size distribution of fully branched cryo-milled starches overlapped with those of native counterparts, suggesting that mechanical cleavage occurs primarily in the interior of AP molecules (inner B-chains).

Further information of the molecular degradation was elucidated by SEC analysis of de-branched starches (Fig. 5). After cryo-milling, increases in the small branches and decreases in the longer branches of AP were observed in the size distribution of debranched MS, PS and G50 HAMS, whereas G80 HAMS showed only minor changes. The results further confirmed that

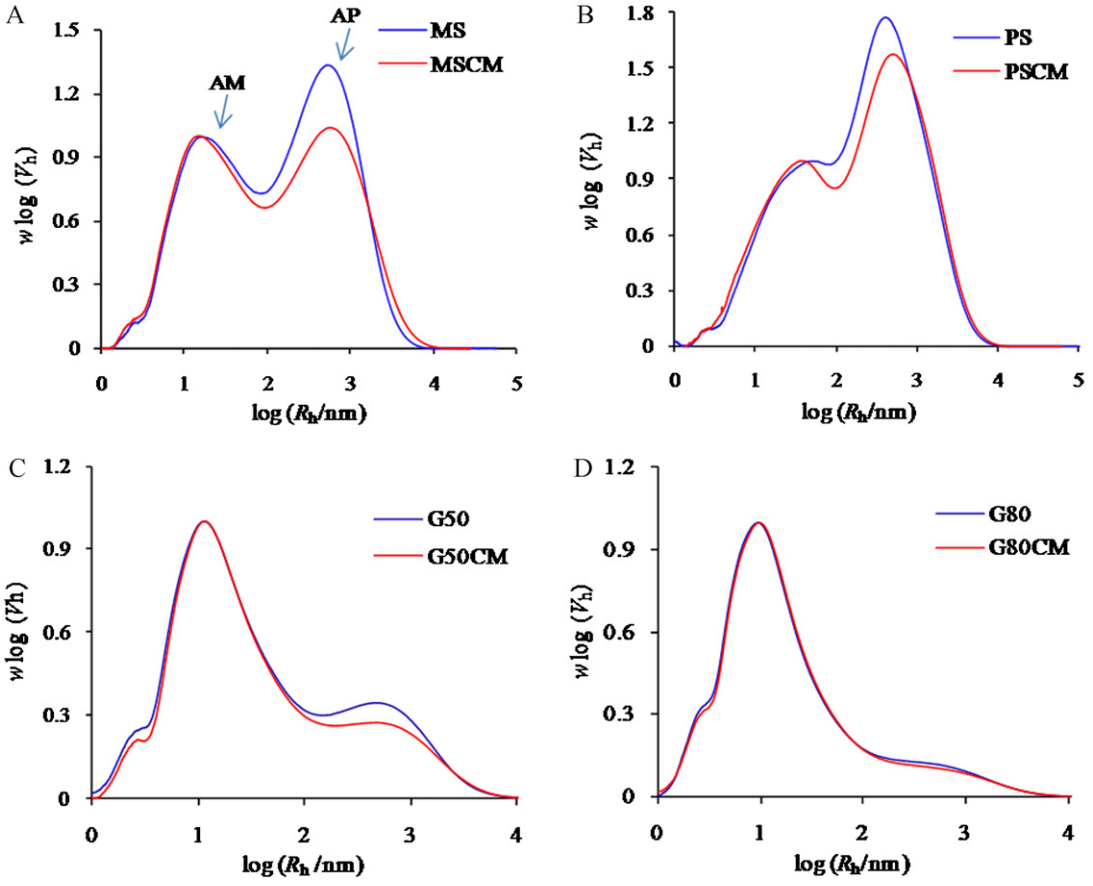

Fig. 4. Molecular size distribution of fully branched (whole) native and cryo-milled starches: MS and MSCM (A); PS and PSCM (B); G50 and G50CM (C); G80 and G80CM (D).

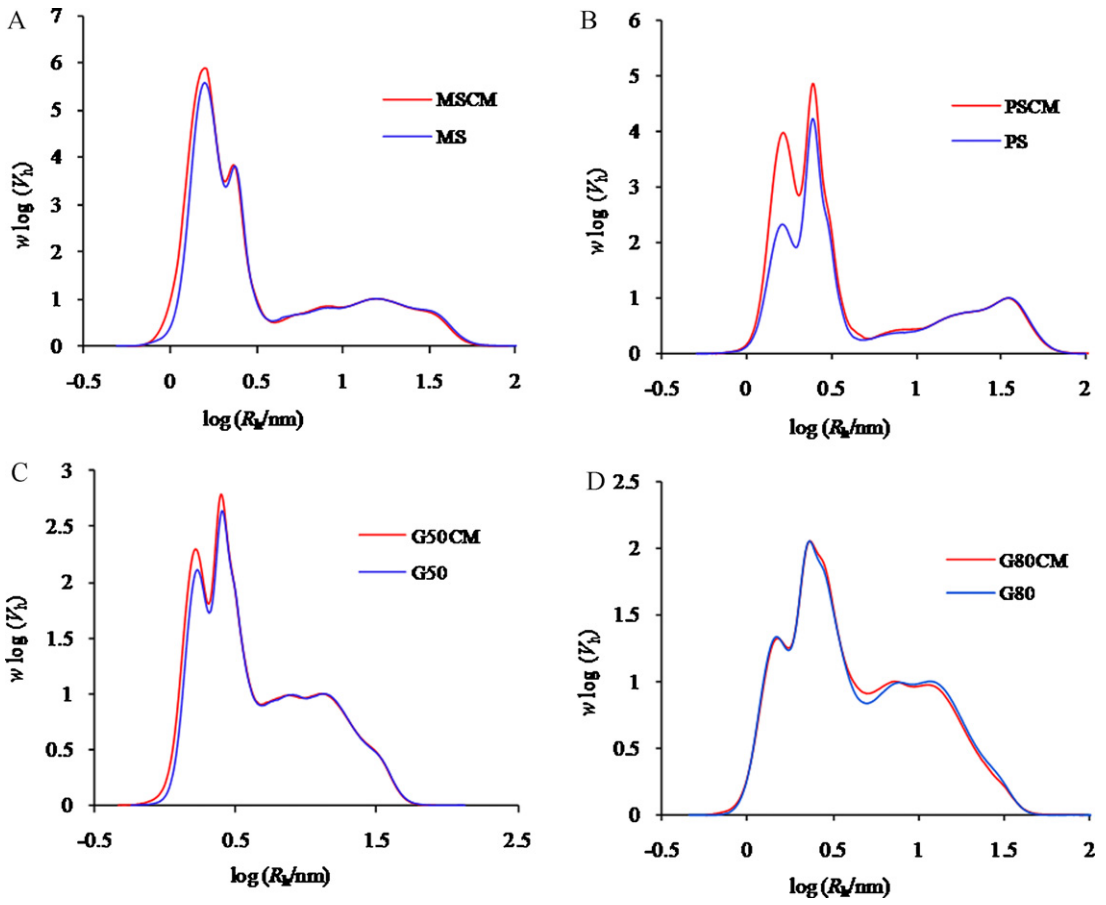

Fig. 5. Molecular size distribution of de-branched native and cryo-milled starches: MS and MSCM (A); PS and PSCM (B); G50 and G50CM (C); G80 and G80CM (D).

the longer branches, corresponding to the amylose fraction, at least for MS and PS, had identical profiles before and after cryo-milling (Fig. 5A and B), consistent with limited degradation of amylose. In the size distribution of de-branched PS (Fig. 5B), there is a greater increase in the very-small branches than those of other starches. As PS has relatively long AP chains with more B2 and B3 chains and fewer A and B1 chains than normal cereal starches (Hizukuri, 1985), it appears that cryo-milling can fracture these longer chains (within lamellae and clusters), which serve as the interior of amylopectin molecules, producing more smaller branches.

The mechanism underlying the loss of double helical structure is possibly due to the unwinding of amylopectin chains by radial splitting along the clusters (Morrison et al., 1994) and is associated with a weaker birefringence pattern (Dhital et al., 2010). The possible mechanisms for the appearance of low molecular weight fractions of AP during milling, such as snapping of AP clusters, breakage of glycosidic bonds in the vicinity of α-1, 6-branching points in the interior of AP molecules, and splitting of granules along radii (i.e. parallel to double helix axes likely to cause molecular breakage) have been described elsewhere (Morrison & Tester, 1994; Morrison et al., 1994; Stark & Yin, 1986; Yin & Stark, 1988).

3.3. Enthalpy transition

Fig. 6 and Table 2 compare the gelatinisation properties between the native and the cryo-milled starches analyzed under heating in excess water conditions. The endotherm for G80 HAMS was very broad and difficult to quantify, and the conclusion temperature might be higher than 120 °C, the maximum tem-

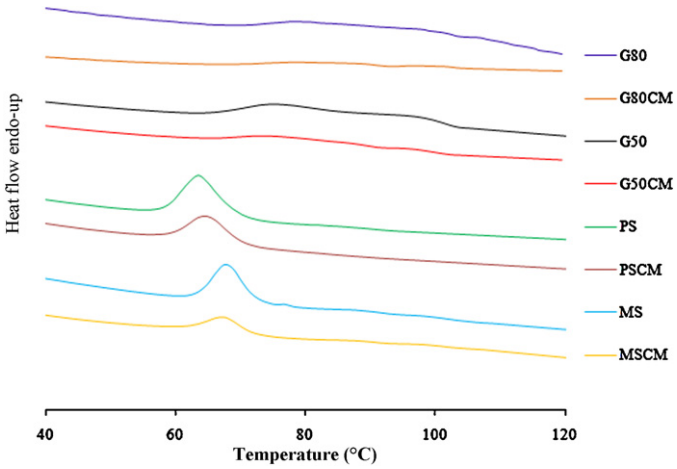

Fig. 6. Differential scanning calorimetry (DSC) thermograms of native and cryo-milled starches.

Table 2
Gelatinisation properties of native and cryo-milled starches.

Starch	ΔH (J/g)[a]	T_o (°C)	T_p (°C)	T_c (°C)
MS	11.4 (0.0)	63.4 (0.1)	67.7 (0.1)	72.1 (0.1)
MSCM	5.7 (0.2)	61.6 (0.0)	67.3 (0.0)	72.0 (0.0)
PS	14.3 (0.3)	58.8 (0.5)	63.7 (0.2)	69.4 (0.2)
PSCM	8.9 (0.1)	59.3 (0.3)	64.6 (0.6)	70.2 (0.0)
G50	15.9 (0.9)	66.1 (0.4)	75.9 (0.1)	99.1 (5.7)
G50CM	8.0 (1.6)	65.8 (0.4)	74.4 (0.9)	91.1 (2.5)

[a] Significant difference ($p < 0.05$) observed between native and cryo-milled starches.

perature used in this experiment, thus it is excluded from the discussion.

Cryo-milling significantly decreased ($p < 0.05$) the enthalpy of gelatinisation (ΔH), whereas the changes in T_o (onset), T_p (peak) and T_c (conclusion) temperatures were insignificant. The endothermic peak associated with starch gelatinisation originates from the disordering of the double helical amylopectin (Cooke & Gidley, 1992). The higher gelatinisation enthalpy of PS compared with that of MS (Table 2) is consistent with the higher amount of double helices in PS than MS (Table 1). Furthermore, the relative decrease in the gelatinisation enthalpy values after cryo-milling (Table 2) is in agreement with the decrease in the content of double helices (Table 1). For example, for MSCM, the content of double helices and gelatinisation enthalpy were 48% and 50%, respectively, of those observed for MS (Tables 1 and 2). Similarly for PSCM, the double helices and gelatinisation enthalpy values were 65% and 62%, respectively, of those observed for PS. For G50 HAMS, the comparable values were 63% and 50%. This provides strong evidence that the disruption of double helices that occurs during the 'dry' cryo-milling process is directly responsible for the reduced gelatinisation measured by heating under excess water conditions.

The insignificant change in the gelatinisation temperatures (T_o, T_p and T_c) between native and cryo-milled starches (Table 2) is consistent with the same molecular structural features (e.g. amylopectin clusters) being present after cryo-milling, i.e. the dominant effect of cryo-milling for 20 min is on molecular conformation, not molecular size. In HAMS, broad endotherms were observed for both native and cryo-milled starches. In particular, the longer amylopectin branch lengths and the likelihood that some amylose in HAMS is present as part of a double helical structure would be expected to require a high temperature and enthalpy to disorder, therefore leading to high gelatinisation temperature and enthalpy (Shi, Capitani, Trzasko, & Jeffcoat, 1998).

4. Conclusions

The effects of cryo-milling on the structure of four diverse granular starches namely maize, potato, Gelose 50 and Gelose 80 starches, having different crystalline polymorphs and percentage of crystallinity were systematically studied using contemporary techniques. The cryo-milled starches had qualitatively similar properties to those of ball-milled starches reported previously (Morrison & Tester, 1994; Morrison et al., 1994; Stark & Yin, 1986; Yin & Stark, 1988) suggesting that milling is predominantly a physical process rather than a thermal process. HAMS granules by virtue of higher amylose content and less ordered structure were more resistant to physical damage than MS and PS, which had less amylose and more ordered structure. Quantitative indices of ordered structure (X-ray crystallinity, helix content by NMR, and gelatinisation enthalpy by DSC) showed that all starches were significantly disrupted by cryo-milling with different measures showing similar relative structure loss values. Molecular size profiles of MS, PS, and G50 before and after de-branching showed some degradation due to cryo-milling, but this was relatively minor, and no changes were detectable for G80 HAMS, despite the significant decreases in the indices of ordered structure in the starch granules. It was, therefore, concluded that cryo-milling disrupted molecular order and molecular size independently, and that the decrease in the molecular size is not a pre-requisite for the loss of ordered structure. The implication is that the mechanical forces acting during cryo-milling are capable of disrupting helical and crystalline structures without breaking the covalent bonds of starch molecules.

Acknowledgements

The University of Queensland Research Scholarship (UQRS), University of Queensland International Research Award (UQIRA), and Australian Research Council (Discovery Grant DP0985694) are acknowledged for their support of this work.

References

Becker, A., Hill, S. E., & Mitchell, J. R. (2001). Milling – A further parameter affecting the rapid visco analyser (RVA) profile. *Cereal Chemistry*, *78*(2), 166–172.

Bulkin, B. J., Kwak, Y., & Dea, I. C. M. (1987). Retrogradation kinetics of waxy-corn and potato starches – A rapid Raman-spectroscopic study. *Carbohydrate Research*, *160*, 95–112.

Cael, J. J., Koenig, J. L., & Blackwell, J. (1975). Infrared and Raman-spectroscopy of carbohydrates. 6. Normal coordinate analysis of V-amylose. *Biopolymers*, *14*(9), 1885–1903.

Cave, R. A., Seabrook, S. A., Gidley, M. J., & Gilbert, R. G. (2009). Characterization of starch by size-exclusion chromatography: The limitations imposed by shear scission. *Biomacromolecules*, *10*(8), 2245–2253.

Chen, J.-J., Lii, C.-Y., & Lu, S. (2003). Physicochemical and morphological analyses on damaged rice starches. *Journal of Food and Drug Analysis*, *11*(4), 283–289.

Cooke, D., & Gidley, M. J. (1992). Loss of crystalline and molecular order during starch gelatinization – Origin of the enthalpic transition. *Carbohydrate Research*, *227*, 103–112.

Devi, A. F., Fibrianto, K., Torley, P. J., & Bhandari, B. (2009). Physical properties of cryomilled rice starch. *Journal of Cereal Science*, *49*(2), 278–284.

Dhital, S., Shrestha, A. K., & Gidley, M. J. (2010). Effect of cryo-milling on starches: Functionality and digestibility. *Food Hydrocolloids*, *24*(2–3), 152–163.

Han, X. Z., Campanella, O. H., Mix, N. C., & Hamaker, B. R. (2002). Consequence of starch damage on rheological properties of maize starch pastes. *Cereal Chemistry*, *79*(6), 897–901.

Hizukuri, S. (1985). Relationship between the distribution of the chain-length of amylopectin and the crystalline-structure of starch granules. *Carbohydrate Research*, *141*(2), 295–306.

Htoon, A., Shrestha, A. K., Flanagan, B. M., Lopez-Rubio, A., Bird, A. R., Gilbert, E. P., et al. (2009). Effects of processing high amylose maize starches under controlled conditions on structural organization and amylase digestibility. *Carbohydrate Polymers*, *75*(2), 236–245.

Huang, Z. Q., Lu, J. P., Li, X. H., & Tong, Z. F. (2007). Effect of mechanical activation on physico-chemical properties and structure of cassava starch. *Carbohydrate Polymers*, *68*(1), 128–135.

Kizil, R., Irudayaraj, J., & Seetharaman, K. (2002). Characterization of irradiated starches by using FT-Raman and FTIR spectroscopy. *Journal of Agricultural and Food Chemistry*, *50*(14), 3912–3918.

Lopez-Rubio, A., Flanagan, B. M., Gilbert, E. P., & Gidley, M. J. (2008). A novel approach for calculating starch crystallinity and its correlation with double helix content: A combined XRD and NMR study. *Biopolymers*, *89*, 761–768.

Morrison, W. R., & Tester, R. F. (1994). Properties of damaged starch granules. 4. Composition of ball-milled wheat starches and of fractions obtained on hydration. *Journal of Cereal Science*, *20*(1), 69–77.

Morrison, W. R., Tester, R. F., & Gidley, M. J. (1994). Properties of damaged starch granules. 2. Crystallinity, molecular order and gelatinization of ball-milled starches. *Journal of Cereal Science*, *19*(3), 209–217.

Santha, N, Sudha, K. G., Vijayakumari, K. P., Nayar, V. U., & Moorthy, S. N. (1990). Raman and infrared-spectra of starch samples of sweet-potato and cassava. *Proceedings of the Indian Academy of Sciences-Chemical Sciences*, *102*(5), 705–712.

Sevenou, O., Hill, S. E., Farhat, I. A., & Mitchell, J. R. (2002). Organisation of the external region of the starch granule as determined by infrared spectroscopy. *International Journal of Biological Macromolecules*, *31*(1–3), 79–85.

Shi, Y. C., Capitani, T., Trzasko, P., & Jeffcoat, R. (1998). Molecular structure of a low-amylopectin starch and other high-amylose maize starches. *Journal of Cereal Science*, *27*(3), 289–299.

Stark, J. R., & Yin, X. S. (1986). The effect of physical damage on large and small barley starch granules. *Starch/Starke*, *38*(11), 369–374.

Syahariza, Z. A., Li, E., & Hasjim, J. (2010). Extraction and dissolution of starch from rice and sorghum grains for accurate structural analysis. *Carbohydrate Polymers*, *82*(1), 14–20.

Tamaki, S., Hisamatsu, M., Teranishi, K., Adachi, T., & Yamada, T. (1998). Structural change of maize starch granules by ball-mill treatment. *Starch/Starke*, *50*(8), 342–348.

Tamaki, S., Hisamatsu, M., Teranishi, K., & Yamada, T. (1997). Structural change of potato starch granules by ball-mill treatment. *Starch/Starke*, *49*(11), 431–438.

Tan, I., Flanagan, B. M., Halley, P. J., Whittaker, A. K., & Gidley, M. J. (2007). A method for estimating the nature and relative proportions of amorphous, single, and double-helical components in starch granules by C-13 CP/MAS NMR. *Biomacromolecules*, *8*(3), 885–891.

Tester, R. F. (1997). Properties of damaged starch granules: Composition and swelling properties of maize, rice, pea and potato starch fractions in water at various temperatures. *Food Hydrocolloids*, *11*(3), 293–301.

Tester, R. F., & Morrison, W. R. (1994). Properties of damaged starch granules. 5. Composition and swelling of fractions of wheat-starch in water at various temperatures. *Journal of Cereal Science*, *20*(2), 175–181.

vanSoest, J. J. G., Tournois, H., deWit, D., & Vliegenthart, J. F. G. (1995). Short-range structure in (partially) crystalline potato starch determined with attenuated total reflectance Fourier-transform IR spectroscopy. *Carbohydrate Research*, *279*, 201–214.

Yamada, M., Tamaki, S., & Hisamatsu, M. (1997). Molecular change of starch granules with physical treatment. Potato starch by ball-mill treatment. In P. J. Frazier, A. M. Donald, & P. Richmond (Eds.), *Starch structure and functionality* (pp. 59–67). Cambridge: The Royal Society of Chemistry.

Yin, X. S., & Stark, J. R. (1988). Molecular modification of barley starch granules by different types of physical treatment. *Journal of Cereal Science*, *8*(1), 17–28.

Zobel, H. F. (1964). X-ray analysis of starch granules. In L. R. Whistler, & R. J. Smith (Eds.), *Methods in carbohydrate chemistry IV* (pp. 109–113). New York: Academic press.